THE EFFECT OF HEAT TRANSFER ON SEPARATION OF LAMINAR COMPRESSIBLE BOUNDARY LAYERS

Thesis by

Stuart B. Savage

In Partial Fulfillment of the Requirements

For the Degree of

Aeronautical Engineer

California Institute of Technology

Pasadena, California

1962

ACKNOWLEDGMENTS

The author wishes to express his appreciation to Professor Lester Lees for his guidance throughout the course of the investigation. The author is indebted to Dr. Barry Reeves for many helpful discussions. Thanks are due to Mrs. Geraldine Van Gieson for her help in preparing the manuscript.

This study is part of a general investigation of separated flows being conducted at GALCIT under AFOSR Contract AF 49(638)-916.

ABSTRACT

Tani's integral method is extended to treat laminar two-dimensional compressible boundary layers with heat transfer and arbitrary pressure gradient for both attached and separated flows. A carefully chosen one-parameter family for the velocity profiles and a "universal" stagnation enthalpy profile are assumed for attached flows. The accuracy of the method is examined by comparing the results with several "exact" numerical solutions and satisfactory agreement is obtained. For separated flows one-parameter families are assumed for both the velocity and stagnation enthalpy profiles. In this case the accuracy of the method is poor; however, suggestions are made as to how it might be improved within the present framework.

TABLE OF CONTENTS

PART		PAGE
	Acknowledgments	ii
	Abstract	iii
	Table of Contents	iv
	List of Figures	vi
	List of Symbols	vii
I.	Introduction	1
II.	Boundary Layer Integral Equations	8
	II. 1. The Stewartson Transformation	8
	II. 2. Integral Form of Equations	11
III.	Velocity and Total Temperature Profiles	13
IV.	Solutions of the Boundary Layer Integral Equations	18
	IV. 1. Attached Flow	18
	IV. 1. 1. Similarity Solutions	18
	IV. 1. 2. Flow with Linearly Decreasing External Velocity in Transformed Plane	19
	IV. 2. Separated Flow	22
	IV. 2. 1. Similarity Solutions	22
V.	Discussion and Future Work	23
	V. 1. Singularity at the Separation Point	23
	V. 2. Velocity Profiles in Separated Region	25
	V. 3. Interaction Between Viscous Flow and External Stream	26

VI. Concluding Remarks 28

References 29

Tables 32

Figures 35

LIST OF FIGURES

NUMBER		PAGE
1	Similarity Separation Velocity Profiles in the Incompressible Plane	35
2	Boundary Layer Functions "f" and "g"	36
3	Similarity Total Temperature Profiles in the Incompressible Plane	37
4	Pressure Gradient Parameter vs. Wall Temperature for Similarity Separation Flow	38
5	Velocity Boundary Layer Characteristics in Incompressible Plane for $S_w = + 1.0$	39
6	Thermal Boundary Layer Characteristics in Incompressible Plane for $S_w = + 1.0$	40
7	Velocity Boundary Layer Characteristics in Incompressible Plane for $S_w = - 0.762$	41
8	Thermal Boundary Layer Characteristics in Incompressible Plane for $S_w = - 0.762$	42
9	Comparison of Velocity and Temperature Profiles for Separated Similarity Flow	43

LIST OF SYMBOLS

a	velocity profile parameter; also speed of sound
b	thermal profile parameter
C_p	specific heat at constant pressure
f, g	boundary layer functions
h	enthalpy
H	form factor, $H = (\delta_i^*/\theta_i)$
k	thermal conductivity
L	arbitrary length
m	exponent in Falkner-Skan external velocity distribution $U_e = CX^m$
m_e , m_∞	$\frac{\gamma - 1}{2} M_e^2$, $\frac{\gamma - 1}{2} M_\infty^2$
M	Mach number
p	static pressure
Pr	Prandtl number, $Pr = \frac{\mu C_p}{k}$
S	total enthalpy function $S = \frac{h_o}{h_{o\infty}} - 1$
T	absolute temperature
u	longitudinal velocity component
U	transformed longitudinal velocity, $U = u\,(a_\infty/a_e) = \psi_Y$
v	normal velocity component
V	transformed normal velocity, $V = -\psi_X$
x	coordinate along surface
X	transformed coordinate along surface, $X = \int_o^x \frac{p_e}{p_\infty} \frac{a_e}{a_\infty}\, dx$
y	normal coordinate
Y	transformed normal coordinate, $Y = \int_o^y \frac{\rho a_e}{\rho_\infty a_\infty}\, dy$

D, E, F	functions of "a" defined by Eq. (31)
G, P	functions of "a" defined by Eqs. (33) and (34)
Q	function of "a" defined by Eq. (32a)
J, W, Z, R	functions of "a" and "b" defined by Eqs. (32b), (32c) and (35)
a	function of "a" defined by Eq. (44)
ϕ, ζ	functions of "a" and "b" defined by Eqs. (45) and (46)
$\mathcal{E}$	total enthalpy defect thickness, $\mathcal{E} = \int_0^{\Delta} S \, d \, Y$
$\mathcal{F}$	total enthalpy-flux thickness, $\mathcal{F} = \int_0^{\Delta} (U/U_e) \, S \, d \, Y$
β	pressure gradient parameter, $\beta = (2m/m+1)$
γ	ratio of specific heats, $\gamma = (C_p/C_v)$
δ	boundary layer thickness
δ^*	displacement thickness
Δ	transformed boundary layer thickness
ε	$M_e - M_\infty$
η	similarity variable, $\eta = (Y/X)\sqrt{\frac{m+1}{2} \frac{U_e X}{\nu_{o\infty}}}$
θ	momentum thickness
θ^*	energy thickness
Θ	streamline direction angle relative to a flat wall (oriented in the free stream direction) at $y = \delta$
Λ, λ	Pohlhausen type parameters defined by Eq. (40)
μ	viscosity
ν	μ/ρ

τ_w	wall shear stress
χ	X/L
ψ	stream function

Subscripts

e	local flow just outside boundary layer
i	transformed quantity in the incompressible plane
w	wall or surface value
0	stagnation value
1	initial value
∞	free stream conditions

I. INTRODUCTION

The phenomenon of flow separation is present in almost all fluid mechanical devices. Its presence is seldom welcomed since it can cause reduced efficiencies, increased drag, buffeting, control surface "buzz", center of pressure shift on cylindrical-flare bodies[1], and many other troublesome effects. In fact, in many cases the onset of separation puts an upper limit on the performance -- the well known "stalling" of an airfoil is a good example of such a limit. On the other hand, there are situations where separated flows may be beneficial, such as for the reduction of drag and heat transfer at hypersonic speeds[2]. Despite the obvious importance of flow separation, the problem has escaped analytic treatment because of its complex nature, and remains a poorly understood and essentially unsolved problem.

Separation may be defined by introducing the concept of a "limiting streamline". Because of the no slip condition, one cannot strictly speak of a streamline "at the wall". At an infinitesimal distance away from the wall, however, the flow has some finite velocity and hence some definable direction. Thus the limiting streamline is given by the limiting flow direction as the wall is approached. Since a streamline cannot end in the fluid it must either pass on downstream to infinity or close in the fluid. Separation is defined as the position at which the limiting streamline leaves the wall and enters the interior of the fluid. Reattachment is defined as the position where the streamline joins either the surface or another fluid streamline. In two dimensional flow, the slope of the limiting streamline at separation and at re-

attachment is defined as $(dy/dx)_{\psi=0} = \lim_{y \to 0} (v/u)$.

The point at which the surface shear stress vanishes also coincides with the separation point in two-dimensional flow. For three-dimensional flows, however, a vanishing shear stress is not a sufficient condition for separation; thus the definition of separation based upon the limiting streamline concept is preferable to that based upon the notion of zero shear stress.

In the usual first order boundary layer theory the required "input" pressure distribution is given by the inviscid external flow. If flow separation is present, however, the flow pattern and hence the pressure distributions can be drastically altered from what they would be were the fluid inviscid. The present boundary layer methods, then, can predict when separation is likely to occur; but if separation does occur, in many cases they give little reliable information about the flow near the separation point and in particular say nothing about the details of the flow behind separation. When the flow is supersonic, the pressure field impressed by the external flow is related to the local inclination of the external flow, which in turn depends on the "upwash" induced by the growth of the boundary layer. Thus the "feedback loop" is closed and in this respect the problem is somewhat simpler than in the subsonic case.

Consider briefly the physical flow situation in a typical supersonic separating and reattaching flow[3]. Sketch A on page 3 shows the flow and the pressure distribution in a compression corner. Typically the separated flow region is characterized by a more or less constant pressure aft of separation followed by a rising pressure just before

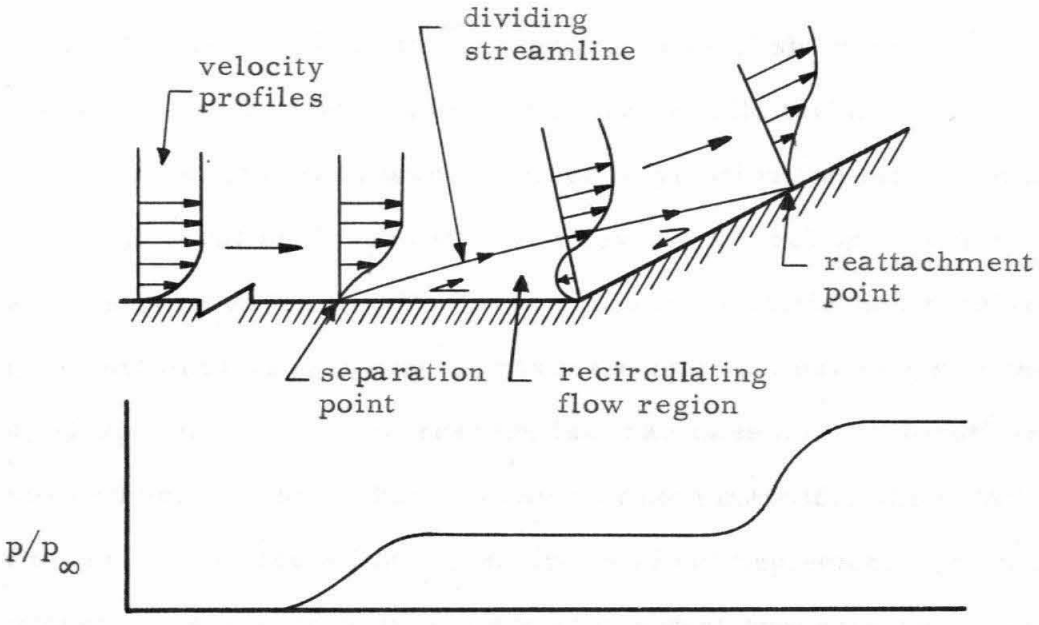

SKETCH A

reattachment. At the separation point the velocity along the limiting or dividing streamline is zero. Because of mixing, as the fluid proceeds downstream, the velocity along the dividing streamline increases. The fluid is thus "prepared" for the reattachment process. It is clear that because of the conservation of mass flow inside the dividing streamline there must be regions of reverse flow. In order for the flow to reattach the fluid along the dividing streamline must be brought to rest and hence the flow must experience a pressure rise prior to reattachment. The whole flow process is a complicated interaction between the external flow and the viscous flow field -- the external flow adjusts itself so as to affect the viscous region in such a way as to achieve reattachment.

Steady flows similar to that just discussed also occur in other shock wave boundary layer interactions[3], behind blunt based bodies in

supersonic flow[4], and near the leading edge of sharp nosed airfoils[5]. The flows can be either wholly laminar, wholly turbulent or "transitional", where transition takes place between separation and reattachment.

Several analyses have been devised to deal with certain supersonic separated flows. The base pressure problem has received a great deal of attention and approximate methods have been developed by Chapman[3], et al. to treat the laminar case and by Korst[6] and his co-workers for the turbulent case. In both methods, the details of the flow in the recirculating region are in effect neglected. The mixing process is assumed to take place at constant pressure and to be the same as that which occurs in the classical free boundary mixing. The analyses are valid when the thickness of the boundary layer at separation is zero. For these cases they are found to predict results which compare favorably with experiment. However, for flows such as the shock-wave boundary layer interaction the upstream boundary layer is of a size comparable to the maximum height from the wall to the dividing streamline after separation, and the analyses break down. In such cases the previous "history" of the boundary layer becomes important and the sizable reverse flow velocities cause the mixing process to depart from the classical free boundary mixing.

The usual one-parameter Kármán-Pohlhausen momentum integral method for attached boundary layer flows and its extension by Thwaites[7], Rott and Crabtree[8], Cohen and Reshotko[9] and others[10-14] is inadequate for separated and reattaching flows. As shown in Sketch A there are regions between separation and reattachment where the static pressure is very nearly constant and reversed flow occurs near

the surface. Since the velocity profile is determined solely by the local pressure gradient in the Kármán-Pohlhausen method, a Blasius-type profile would be obtained for the pressure "plateau" region if the Pohlhausen quartic is employed. The reversed-flow profiles found by Stewartson[15] along the "lower branch" of the Falkner-Skan solution were incorporated into the Thwaites method by Curle[13], but it is not clear that this special family provides the required flexibility. Curle's computed pressure distributions do not show the inflection in pressure as evidenced by experiments.

In an attempt to "unhook" the velocity profile from the local pressure gradient Crocco and Lees[16] introduced a new momentum integral method in which the profile is determined by a single independent shape parameter not explicitly related to the pressure gradient. The Crocco-Lees method has been developed quite extensively[17, 18], and has been used to calculate such problems as shock-wave boundary layer interactions, yielding fairly good results. The main drawback of the method is that it relies upon a mixing coefficient that is not well known for separated flows.

Some of the arbitrary features of the Crocco-Lees method can be eliminated by adopting and extending the two-moment method developed by Tani[19] for attached boundary layers. In this scheme the velocity profile is still determined by a single parameter, say the non-dimensional slope at the surface, a(x), but this parameter is independent of the Thwaites-Pohlhausen pressure gradient parameter $\lambda(x) = \frac{\theta^2}{\nu} \frac{dU_e}{dX}$. The development of the boundary layer is determined by integrating the two simultaneous first order differential equations for a(x) and $\lambda(x)$

obtained by taking the integrals of momentum and mechanical energy across the layer.

Lees and Reeves[20] applied this promising method to adiabatic separated flows. The purpose of the present study is to extend this scheme to the more general case of arbitrary heat transfer at the surface. Theoretical analyses of heat transfer in separated regions have been limited both in scope and in number. Chapman[21] examined the effects of heat transfer and mass injection; however, the laminar layer was required to be thin and at constant pressure. Carlson's[22] theory is one of the few that considered reverse flow velocity profiles, but this analysis too was for constant pressure. Curle[13] treated the shock-wave boundary layer interaction; however, when heat transfer was present this method gave rather poor results for the prediction of separation,and its accuracy in the separated flow region has not been established.

It is well known that surface heat transfer can have a large effect on the behavior of attached boundary layers. For instance, in a positive pressure gradient cooling the surface delays separation and heating the surface moves separation upstream. One of the objectives of the present investigation is to determine the extent to which the effect of surface cooling persists in separated and reattaching flow regions. This effect could be significant in determining the Mach number along the dividing streamline and hence, the extent of the separated-reattaching flow itself[23].

In the interest of simplicity only steady two dimensional laminar boundary layers are considered here. The flow up to the separation

point is treated first and results from the approximate analysis are compared with some "exact" solutions. Tani's[19] method is generalized by representing the velocity profiles as a weighted mean of the Blasius and the average of the non-adiabatic similarity separation profiles, rather than a quartic. The weighting parameter is again the non-dimensional slope at the surface. The analysis is developed to deal with the flow beyond separation and one example is briefly considered.

Only cases for which the external velocity is prescribed are computed. The present study is, however, a preparation for treating the interaction between the viscous layer and the external flow.

II. BOUNDARY LAYER INTEGRAL EQUATIONS

II. 1. The Stewartson Transformation

The equations of the steady laminar two-dimensional compressible boundary layer for perfect fluids are:

Continuity:

$$\frac{\partial}{\partial x}(\rho u) + \frac{\partial}{\partial y}(\rho v) = 0 \tag{1}$$

Momentum:

$$\rho u \frac{\partial u}{\partial x} + \rho v \frac{\partial u}{\partial y} = -\frac{\partial p}{\partial x} + \frac{\partial}{\partial y}\left(\mu \frac{\partial u}{\partial y}\right)$$
$$0 = -\frac{\partial p}{\partial y} \tag{2}$$

Energy:

$$\rho u \frac{\partial h}{\partial x} + \rho v \frac{\partial h}{\partial y} = u \frac{\partial p}{\partial x} + \frac{\partial}{\partial y}\left(\frac{\mu}{P_r} \frac{\partial h}{\partial y}\right) + \mu \left(\frac{\partial u}{\partial y}\right)^2 \tag{3}$$

It is assumed that these equations are valid for the flow beyond separation as well as for the attached flow. There has been some question raised as to whether or not the full Navier Stokes equations are required at the separation point. Oswatitsch[24] demonstrated that a regular solution of the Navier-Stokes equations exists in the neighborhood of the separation point.* In fact, results identical to his are obtained if only the usual boundary layer terms are kept. Thus by using integral methods it should be possible to pass through this region without too much difficulty. The assumption of negligible normal pressure gradients for the separated flow seems to be a reasonable one, except possibly in

---

* The special singular solution found by Goldstein[25] may not be the one that occurs in nature.

certain cases near reattachment where the curvature of the external streamlines is large.

For simplicity the viscosity law is taken to be

$$\frac{\mu}{\mu_\infty} = \frac{T}{T_\infty} \tag{5}$$

As shown by Cohen and Reshotko[9], Eqs. (1), (2), and (3) may be transformed into the form of the two dimensional incompressible laminar boundary layer equations by means of Stewartson's transformation[26], even when the flow is not adiabatic.

A stream function is defined

$$\psi_y = \frac{\rho u}{\rho_\infty}$$

$$\psi_x = -\frac{\rho v}{\rho_\infty} \tag{6}$$

and the following variables are introduced:

$$dX = \frac{a_e}{a_\infty}\frac{\rho_e}{\rho_\infty}\,dx \tag{7}$$

$$dY = \frac{a_e}{a_\infty}\frac{\rho}{\rho_\infty}\,dy \tag{8}$$

The transformed incompressible co-ordinates are denoted by upper case letters X and Y. The subscript e refers to conditions at the edge of the boundary layer, where the flow is assumed to be isentropic, and the subscript ∞ refers to conditions in the free stream. By using Eq. (5) and the assumptions that C_p is constant and that Pr = 1, the following equations are obtained for the flow in the incompressible plane:

$$\frac{\partial U}{\partial X} + \frac{\partial V}{\partial Y} = 0 \tag{9}$$

$$U \frac{\partial U}{\partial X} + V \frac{\partial U}{\partial Y} = U_e \frac{\partial U_e}{\partial X} (1+S) + \nu_\infty \frac{\partial^2 U}{\partial Y^2} \tag{10}$$

$$U \frac{\partial S}{\partial X} + V \frac{\partial S}{\partial Y} = \nu_\infty \frac{\partial^2 S}{\partial Y^2} \tag{11}$$

where S is a dimensionless enthalpy defined by

$$S = \frac{h_o}{h_{oe}} - 1 \tag{12}$$

and h_o is the local stagnation enthalpy.

The stream function has been replaced by the transformed velocities (U, V) defined by

$$U = \psi_Y$$
$$V = -\psi_X \tag{13}$$

and the resulting relation between the transformed and the physical longitudinal velocities is

$$U = \frac{a_\infty}{a_e} u$$

Eqs. (9) - (11) are subject to the following boundary conditions:

$$U(X, 0) = 0$$
$$V(X, 0) = 0$$
$$S(X, 0) = S_w = \text{constant} \tag{14}$$
$$\lim_{Y \to \infty} S = 0$$
$$\lim_{Y \to \infty} U = U_e(X)$$

II. 2. Integral Form of Equations

When Pr = 1 it seems reasonable to assume that the velocity (momentum) and the thermal boundary layers are of the same thickness. Then integrating Eqs. (10) and (11) across the boundary layer between Y = 0 and Y = Δ and making use of Eq. (9) the following momentum and energy integral equations are obtained

$$U_e \frac{d\theta_i^2}{dX} + 2\left(2 + H + \frac{\mathcal{E}}{\theta_i}\right)\theta_i^2 \frac{dU_e}{dX} = \frac{2\theta_i \nu_\infty}{U_e}\left(\frac{\partial U}{\partial Y}\right)_{Y=0} \tag{15}$$

$$U_e \frac{d\mathcal{E}^2}{dX} + 2\mathcal{E}^2 \frac{dU_e}{dX} = -2\nu_\infty \mathcal{F}\left(\frac{\partial S}{\partial Y}\right)_{Y=0} \tag{16}$$

Following Tani[19], the momentum equation, Eq. (10), is multiplied by U and integrated across the boundary layer to obtain the first moment of the momentum equation:

$$U_e \frac{d\theta_i^{*2}}{dX} + 2\left(3 + \frac{2\mathcal{E}}{\theta_i^*}\right)\theta_i^{*2} \frac{dU_e}{dX} = \frac{4\nu_\infty}{U_e^2}\theta_i^* \int_0^\Delta \left(\frac{\partial U}{\partial Y}\right)^2 dY \tag{17}$$

The boundary layer characteristics in the incompressible plane, such as the displacement thickness δ_i^*, the momentum thickness θ_i, the energy thickness θ_i^*, the enthalpy thickness $\mathcal{E}$, and the enthalpy flux thickness $\mathcal{F}$, are defined as follows:

$$\delta_i^* = \int_0^\Delta \left(1 - \frac{U}{U_e}\right) dY \tag{18}$$

$$\theta_i = \int_0^\Delta \frac{U}{U_e}\left(1 - \frac{U}{U_e}\right) dY \tag{19}$$

$$\theta_i^* = \int_0^{\Delta} \frac{U}{U_e}\left(1 - \frac{U^2}{U_e^2}\right) dY \tag{20}$$

$$\xi = \int_0^{\Delta} S\, dY \tag{21}$$

$$\mathcal{E} = \int_0^{\Delta} \frac{U}{U_e} S\, dY \tag{22}$$

Eqs. (15) - (22) have been given in similar form by Poots[27].

Through Stewartson's transformation the various boundary layer characteristic thicknesses in the physical plane may be related to those in the incompressible plane. Thus

$$\delta^* = \int_0^{\delta} \left(1 - \frac{\rho u}{\rho_e u_e}\right) dy = \frac{a_\infty \rho_\infty}{a_e \rho_e}\left[(1+m_e)(\xi + \delta_i^*) + m_e \theta_i\right] \tag{23}$$

$$\theta = \int_0^{\delta} \frac{\rho u}{\rho_e u_e}\left(1 - \frac{u}{u_e}\right) dy = \frac{a_\infty \rho_\infty}{a_e \rho_e}\theta_i \tag{24}$$

$$\theta^* = \int_0^{\delta} \frac{\rho u}{\rho_e u_e}\left(1 - \frac{u^2}{u_e^2}\right) dy = \frac{a_\infty \rho_\infty}{a_e \rho_e}\theta_i^* \tag{25}$$

$$\theta^{**} = \int_0^{\delta} \frac{\rho u}{\rho_e u_e}\left(\frac{T}{T_e} - 1\right) dy = \frac{a_\infty \rho_\infty}{a_e \rho_e}\left[(1+m_e)\mathcal{E} + m_e \theta_i^*\right] \tag{26}$$

where

$$m_e = \frac{\gamma - 1}{2} M_e^2 \tag{27}$$

III. VELOCITY AND TOTAL TEMPERATURE PROFILES

Following Tani[19], Poots[27] expressed the velocity and total temperature profiles as fourth degree polynomials. For each profile, four of the coefficients were determined by fitting the boundary conditions at the wall and the edge of the boundary layer. The remaining coefficient (identified with the gradient at the wall) for each layer was used to characterize the shape of the profile. Thus the velocity and temperature profiles are each members of a separate one-parameter family. The development of these profiles along the surface and the growth of θ_i (or $\frac{\theta_i^2}{\nu_\infty}\frac{dU_e}{dX}$) is found by integrating the three simultaneous differential equations, Eqs. (15) - (17).

In the present paper it is also assumed that the profiles can be expressed as members of one-parameter families. However, the profile shapes were determined in a somewhat different manner, because the use of Tani's quartic for the velocity profile was found to lead to large errors near separation for the case of the cold walls. (This point is discussed further in Section IV. 1. 1.)

Cohen and Reshotko[28] present similar Falkner-Skan type solutions (i. e., when $U_e = CX^m$) for the laminar compressible boundary layer with heat transfer. When the separation profiles in the transformed plane for various values of S_w are normalized and compared, these velocity profiles do not collapse to one universal curve (Figure 1). Thus it would appear that at least two parameters are required to represent the profiles for the general case of an arbitrary S_w. The addition of a second parameter would require the addition of another

differential equation (for example the second moment of the momentum equation) in order to solve the flow problem.* However, to avoid the added complexity of a second parameter, a kind of "mean" one-parameter velocity profile to be used for all S_w was chosen in the following way:

The velocity profile is written as $\frac{U}{U_e} = f(Y/\Delta) + a(X)\, g(Y/\Delta)$, where a is identified with the gradient at the wall. Thus when $a = 0$, $U/U_e = f(Y/\Delta)$, i.e., the separation profile. The function $f(Y/\Delta)$ was determined by taking, in a sense, the "average" of the exact similarity separation profiles from Reference 28 for various values of S_w. The representative average profile chosen for $f(Y/\Delta)$ was the same as the exact separation profile for $S_w = -0.8$, except for slight modification in order that the boundary layer have finite thickness.

For $a = a_{BL}$, the velocity profiles in the transformed plane for all values of S_w reduce to the Blasius profile. Thus, $a_{BL}\, g(Y/\Delta) = (U/U_e)_{BL} - f(Y/\Delta)$, where the subscript BL refers to the "Blasius" values. Since "a" corresponds to the gradient at the wall, the function $g(Y/\Delta)$ was then determined. Explicitly,

$$\left(\frac{\partial (U/U_e)_{BL}}{\partial (Y/\Delta)}\right)_{Y/\Delta=0} = f'(0) + a_{BL}\, g'(0) \quad .$$

By definition $f'(0) = 0$, and g was chosen such that $g'(0) = 1$. For the profiles as chosen, $a_{BL} = 1.99$. The functions $f(Y/\Delta)$ and $g(Y/\Delta)$ are

---

* Based on the similar solutions, this second parameter could instead be determined as a function of S_w and thus the additional differential equation would not be required. This approach would make the tabulation of the boundary layer functions defined by Eqs. (31) - (35) very involved.

given in Table 1 and are shown in Figure 2. This one-parameter family is used to describe the velocity profiles in the separated flow region as well as for attached flow.

Cohen and Reshotko[28] present total temperature profiles in the incompressible transformed plane for various values of S_w and pressure gradient parameter β. If these profiles are "normalized" by "scaling" the normal distance from the wall so that all profiles have the same gradient at the wall, upon comparison an interesting result is obtained. (Figure 3 shows the profiles at separation for various S_w compared with the "flat-plate" profile.) As long as the flow is attached the S/S_w profiles can be represented quite well by one "universal" curve. This universal curve is given by Crocco's integral of the energy equation for the flat plate, namely, $S/S_w = 1 - (U/U_e)_{BL}$, where $(U/U_e)_{BL}$ is the "Blasius" profile. Thus, for attached flow the thermal profile is taken as $S/S_w = \left[1 - \left\{f(Y/\Delta) + a_{BL}\, g(Y/\Delta)\right\}\right]$. In the separated flow region the thermal profiles can no longer be represented by this "universal" profile. The separated thermal profiles are assumed to be the one-parameter family,

$$S/S_w = \left\{1 - f(Y/\Delta)\right\} + b(X)\, g(Y/\Delta) \quad ,$$

where for convenience $f(Y/\Delta)$ and $g(Y/\Delta)$ are the same functions as those used for the velocity profiles.

Summarizing, the velocity profile for both attached flow and separated flow (as long as the height of the reverse flow region is not too large) is taken as

$$U/U_e = f(Y/\Delta) + a(X)\; g(Y/\Delta) \quad . \tag{28}$$

For attached flow the "universal" thermal profile is used

$$S/S_w = \left\{1 - f(Y/\Delta)\right\} - 1.99\, g(Y/\Delta) \quad , \tag{29}$$

i.e., $b = -1.99$, while for separated flow the thermal profile is given by

$$S/S_w = \left\{1 - f(Y/\Delta)\right\} + b(X)\; g(Y/\Delta) \tag{30}$$

Now that the profile shapes are decided upon, Eqs. (18) - (22) can be integrated graphically to give the various non-dimensionalized boundary layer thicknesses in terms of a and b. Thus

$$(\delta_i^*)/\Delta = .4204 - .0651a = D \tag{31a}$$

$$(\theta_i)/\Delta = .09080 + .02616a - .00842a^2 = E \tag{31b}$$

$$\theta_i^*/\Delta = .1368 + .0360a - .00655a^2 - .001182a^2 = F \tag{31c}$$

$$(\Delta/U_e^2) \int_0^{\Delta} (\partial U/\partial Y)^2\, dY = 1.763 - .5040a + .2068a^2 = (Q/4F) \tag{32a}$$

$$\mathcal{E}/S_w\Delta = .4204 + .0651b = W \,.\, E \tag{32b}$$

$$\mathcal{F}/S_w\Delta = .0908 + .0456a + .01947b + .00842ab \tag{32c}$$

$$= J \,.\, E = Z \,.\, F \quad ,$$

where $J = (\mathcal{E}/S_w\theta_i)$ and $Z = (\mathcal{E}/S_w\theta_i^*)$;

$$H = D/E \quad , \quad G = F/E \tag{33}$$

$$(2\theta_i/U_e)\,(\partial U/\partial Y)_{Y=0} = P = 2aE \tag{34}$$

$$-(2\mathcal{F}/S_w^2)\,(\partial S/\partial Y)_{Y=0} = R = -2b\, J \,.\, E = -2bZ \,.\, F \tag{35}$$

The quantities given by Eqs. (31) - (35) are functions of a and b only and their numerical values are tabulated in Table 2.

Eqs. (15) - (17) are now rewritten in the form

$$U_e \frac{d\theta_i^2}{dX} + 2(2 + H + S_w W)\,\theta_i^2 \frac{dU_e}{dX} = \nu_\infty P \tag{36}$$

$$U_e \frac{d(G^2\theta_i^2)}{dX} + 2G^2\theta_i^2(3 + 2S_w Z)\frac{dU_e}{dX} = \nu_\infty Q \tag{37}$$

$$U_e \frac{d(J^2\theta_i^2)}{dX} + 2J^2\theta_i^2 \frac{dU_e}{dX} = R \tag{38}$$

Given the external velocity $U_e = U_e(X)$, the wall temperature and the initial conditions, the set of first order differential equations, Eqs. (36) - (38), can now be solved for the three unknown functions $a(X)$, $b(X)$, and $\theta_i(X)$.

IV. SOLUTIONS OF THE BOUNDARY LAYER INTEGRAL EQUATIONS

IV. 1. Attached Flow

For attached flow, the "universal" S/S_w profile is used and thus "b" is constant and numerically equal to -1.99. The problem is simplified and reduced to solving the two first order differential equations, Eqs. (36) and (37).

IV. 1. 1. Similarity Solutions

When the flow is a similar Falkner-Skan type flow (i.e., when $U_e = CX^m$) a = const. and Eqs. (36) and (37) reduce to two algebraic equations. Because of the way in which the velocity and temperature profiles were chosen the errors in the solution of the integral equations are largest for a similar flow which is always on the verge of separation (i.e., a = 0). For this case values of the pressure gradient parameter, $\beta = (2m/m+1)$, were calculated for various values of S_w. Figure 3 shows a plot of $\beta_{separation}$ vs. S_w calculated by the present method compared with exact solutions obtained by Cohen and Reshotko[28].

It should be mentioned that initially Tani's quartic was chosen for the velocity profile and a one-parameter cubic was chosen for the thermal profile. The full set of equations, Eqs. (36), (37), and (38), were solved for $\beta_{separation}$ vs. S_w. This curve is also shown in Figure 4, and it can be seen that when these profile shapes are used the integral method is in considerable error for cold walls. This error is mainly caused by the large difference between Tani's quartic velocity profile and the exact profiles at separation. For this reason

the profile shapes were determined as stated in Section III, resulting in improved accuracy for the cold wall. The qualitative shape of the exact $\beta_{separation}$ vs S_w curve is not matched by the integral method. Near $S_w = -1.0$ the exact curve has negative curvature whereas with only a one-parameter family for the velocity profiles the integral method gives positive curvature everywhere. However, the present method gives values fairly close to the exact solution except at $S_w = -1.0$.

The displacement, momentum and enthalpy thicknesses and the gradient of S/S_w at the wall were calculated by the present method for the separation profile. These data compared with the exact results from Reference 28 are shown in Table 3.

The comparison is favorable except for the displacement thickness at $S_w = -1.0$ (highly cooled wall) where the errors brought about by the one-parameter velocity profile show up rather strongly.

Again it is repeated that the errors in the present method will most likely be greatest for this case of "incipient separation".

IV. 1. 2. Flow with Linearly Decreasing External Velocity in Transformed Plane

Calculations have been carried out for the case of a linearly decreasing velocity in the incompressible plane, i. e.,

$$U_e = U_1 \left(1 - \frac{X}{L}\right) \tag{39}$$

where U_1 is the velocity at $X = 0$ and L is some characteristic length.

A Pohlhausen type parameter is introduced

$$\Lambda = G^2 \lambda = \frac{G^2 \theta_i^2}{\nu_\infty} \frac{dU_e}{dX} \tag{40}$$

Using Eqs. (39) and (40), after some manipulation Eqs. (36) and (37) may be put in the following form suitable for numerical integration

$$\frac{d\Lambda}{d\mathcal{X}} = \frac{1}{(1-\mathcal{X})}\left[\mathcal{S}\Lambda - Q\right] \tag{41}$$

$$\frac{d\ell n G}{d\mathcal{X}} = \frac{1}{(1-\mathcal{X})}\left[\frac{\alpha}{\Lambda} + \phi\right] \tag{42}$$

where

$$\mathcal{X} = X/L \tag{43}$$

$$\alpha = (EG^2 a - \frac{Q}{2}) \tag{44}$$

$$\phi = (1 + 2\,S_w\,Z - H - S_w\,w) \tag{45}$$

$$\mathcal{S} = (6 + 4\,S_w\,Z) \tag{46}$$

Now α, ϕ, and $\mathcal{S}$ are functions only of a. Eqs. (41) and (42) may be solved by eliminating X and numerically integrating the single resulting differential equation in the Λ - ℓn G plane, and then by a simple quadrature transforming to the X plane. A solution may also be obtained by numerically solving Eqs. (41) and (42) simultaneously and this second method was used here.

Eqs. (41) and (42) are subject to the initial condition that

$$\Lambda = 0 \quad \text{at} \quad X = 0 \tag{47}$$

The numerical integration was started by the Runge-Kutta method and continued by Milnes method[29]. As Tani[19] and Poots[27] found with a uniformly retarded external velocity it was difficult to carry out the solution right up to the separation point because of the rapid growth of ($d\ell nG/d\mathcal{X}$) near separation. (The behavior near separation is discussed in Section V. 1.) However, the solution was carried out to X = 0. 56 and

extrapolated from there to separation.

From the numerical computation, values of a and Λ are obtained for various values of X. Using this information the boundary layer characteristics in the incompressible plane such as δ_i^*, θ_i, θ_i^*, $\mathcal{E}$, $\tilde{\mathcal{E}}$, $(\partial S/\partial Y)_{Y=0}$ and $(\partial U/\partial Y)_{Y=0}$ can be calculated.

Using the Hartree-Womersley method Poots[27] obtained an "exact" numerical solution for the above case of $S_w = 1.0$ and a linearly decreasing external velocity (taking $U_1 = 1$ and $L = 8$ to simplify the numerical calculations). Poots also presented the results of an integral method which amounted to solving the set of three differential equations, Eqs. (36) - (38), using Tani's quartic for the velocity profile and a similar quartic for the total temperature profile. Calculations by the present method compare favorably with the exact solution of Poots[27] as shown in Figures 5 and 6. The present integral method is somewhat less accurate, but also simpler than the integral method of Poots. It is also expected that the present method might be more accurate than the integral method of Poots for the more interesting case of a cold wall since the present velocity profiles are probably more realistic than those represented by Tani's quartic.

For comparison purposes, the boundary layer properties for the case of a cold wall with the wall temperature equal to the initial temperature of the external stream, i.e., $S_w = -0.762$ were computed by the present method. These results are shown in Figures 7 and 8.

The present method for a non-adiabatic wall predicts that the heat transfer rate at separation is finite. Analyses such as Curle's[13] which express the temperature profiles as power series of the velocity

ratio, U/U_e, incorrectly yield zero heat transfer at separation and can also reverse the sense of the wall temperature gradient in the reverse flow region.

IV. 2. Separated Flow

For separated flow it is no longer possible to use the "universal" S/S_w profile and the full set of differential equations, Eqs. (36), (37), and (38) must be solved.

IV. 2. 1. Similarity Solutions

Again for the similar type flows, Eqs. (36), (37), and (38) reduce to a set of simultaneous algebraic equations. These equations were solved for the particular case of $S_w = -0.8$ and $\beta = -0.10$. The velocity and temperature profile were computed and are compared in Figure 9 with the exact solution of Cohen and Reshotko[28]. The various integral thicknesses were not calculated in Reference 28 and thus no comparison is made. However, as can be seen from Figure 9 the comparison of the profile shapes is rather poor and the present integral method gives only very rough estimates of such things as skin friction and wall heat transfer rates. The reason for these discrepancies lies in the inability of the assumed form of the velocity profile to match the exact profile shape.

V. DISCUSSION AND FUTURE WORK

V. 1. Singularity at the Separation Point

The present method points out rather simply some interesting features that occur near the separation point. Eliminating $(d\theta_i^2/dX)$ from Eqs. (36) and (37) one obtains

$$\frac{dG^2}{dX} = 2G\frac{dG}{da}\frac{da}{dX} = \frac{G^2}{\Lambda U_e}\frac{dU_e}{dX}\left[Q - G^2P + 2\Lambda\left\{H-1+S_w(W-2Z)\right\}\right] \tag{48}$$

Near separation, as $a \longrightarrow 0$, G(a) goes through a minimum, i.e., $(dG/da) = 0$. Thus when (da/dX) is finite and $(dG/da) = 0$, a unique value is obtained for Λ, i.e., $\Lambda = \Lambda^\circ$. However, for example, in the case of a uniformly retarded external velocity (Section IV. 1. 2.) when Eqs. (41) and (42) are integrated, it is found that a value of Λ is reached before separation such that $\Lambda < \Lambda^\circ$ (algebraically). From Eq. (41) it can be seen that $(d\Lambda/dX) < 0$ for all X up to separation. Thus, when $(dG/da) = 0$, $\Lambda \neq \Lambda^\circ$, which implies that $(da/dX) = -\infty$, and a singularity occurs at this point. It is found that when (da/dX) at separation is infinite, $(d\delta^*/dX)$ is also infinite; however, $(d\theta_i/dX)$ and $(d\theta_i^*/dX)$ remain finite. Examining the wall shear stress

$$\tau_w = \left(\mu\frac{\partial u}{\partial y}\right)_{y=0} \sim \frac{aU_e}{\Delta}$$

$$\frac{d\tau_w}{dX} \sim \frac{U_e}{\Delta}\frac{da}{dX} + \frac{a}{\Delta}\frac{dU_e}{dX} - \frac{U_e a}{\Delta^2}\frac{d\Delta}{dX} \tag{49}$$

and since

$$\frac{d\Delta}{dX} \sim \frac{1}{a}$$

$$\left(\frac{d\tau_w}{dX}\right)_{a\to 0} \sim \frac{da}{dX} \tag{50}$$

Keeping first order terms near separation, it can be shown easily from Eq. (48) that

$$a \sim (X_{\text{separation}} - X)^{\frac{1}{2}} \quad , \quad \text{thus } (\partial u/\partial y)_{y=0} \sim (X_{\text{separation}} - X)^{\frac{1}{2}}$$

as assumed by Goldstein[25] near the separation point. As Goldstein found, for this special type of external velocity distribution (when $(d^2U_e/dX^2) \leq 0$) the solution cannot be continued downstream of the separation point.

Prandtl[30] and later Meksyn[31, 32] showed that the pressure distribution in the region of separation cannot be chosen arbitrarily but must satisfy certain conditions compatible with the reverse flow region downstream of separation. Prior to separation Λ must go through a minimum and near separation $(d^2U_e/dX^2) > 0$. This condition is evident from the integral form of the equations, if one takes Eq. (40) and examines the conditions for $(d\Lambda/dX)$ to change sign, in order that Λ pass through $\Lambda = \Lambda^\circ$ at separation.

While the special class of flows where $(d^2U_e/dX^2) \leq 0$ (right up to the separation point) lead to a singularity at separation and cannot be carried downstream, exact solutions for such cases are nevertheless of interest for checking approximate methods.

V. 2. Velocity Profiles in Separated Region

Examination of the solutions of the Falkner-Skan equation shows that along the lower branch,[15] the maximum backflow velocity is zero at separation, reaches a maximum as β increases algebraically and then decreases to zero again as $\beta \longrightarrow 0$. The displacement thickness increases without limit as $\beta \longrightarrow 0$ along the lower branch (i. e., at $\beta = 0$ the profile is the classical free boundary mixing problem for zero pressure gradient). Clearly such a behavior cannot be reproduced by the kind of one-parameter velocity profile chosen in the present paper. The need for such a behavior is illustrated by some work of Reeves* for the shock-wave boundary layer interaction on an adiabatic flat plate. Reeves used Tani's quartic for the velocity profile and included a third integral moment equation to relate the pressure gradient to the displacement effect of the boundary layer. It was found that the pressure did not level off into the usual "plateau" region but reached a maximum and then decreased before rising again at reattachment. The velocity profile was such that the displacement thickness could not grow fast enough to obtain the pressure "plateau".

Thus it would appear that for the reverse flow region it may be necessary either to use a two-parameter velocity profile or to use two or more layers. Another simpler and promising method has been suggested by Professor L. Lees. A one-parameter family of velocity profiles could be constructed based upon the "lower branch" Falkner-Skan solutions. It should be noted that it is not necessary to relate the

---

* private communication

parameter to any pertinent physical quantity, but only that the profiles be denoted by this single parameter in such a way that the integral properties may be tabulated (as in Table 2).

V. 3. Interaction Between Viscous Flow and External Stream

For all the examples computed here the external velocity gradient was assumed to be given. In a problem such as the shock wave boundary layer interaction the external velocity is not known a priori and the interaction between the viscous flow and the external stream must be determined. The following equation is obtained by applying the Stewartson transformation to the continuity equation and integrating across the boundary layer

$$\frac{\tan \Theta}{1+m_\infty} = \theta_i \frac{dH}{dX} + \left[H + \frac{m_e}{1+m_e}\right]\frac{d\theta_i}{dX} + \frac{d\bar{\xi}}{dX} + \frac{m_e}{1+m_e}\left[2\left(1+\frac{\bar{\xi}}{\theta_i}\right)\right.$$

$$\left. + \left(\frac{3\gamma-1}{\gamma-1}\right)H + \left(\frac{\gamma+1}{\gamma-1}\right)\left(\frac{m_e}{1+m_e} + \frac{\bar{\xi}}{\theta_i}\right) + \frac{M_e^2-1}{m_e(1+m_e)}\frac{1}{\theta_i}\int_0^\Delta \frac{U}{U_e}\,dY\right]\frac{\theta_i}{M_e}\frac{dM_e}{dX} \tag{51}$$

where Θ = streamline direction angle relative to a flat wall (oriented in the free stream direction) at $y = \delta$,

$\tan \Theta = \frac{V_e}{U_e}$

$m_\infty = \frac{\gamma-1}{2} M_\infty^2$

And for example, when $\Theta << 1$, $\tan \Theta \simeq \Theta$ in Eq. (51) and the

linearized Prandtl-Meyer equation gives

$$\textcircled{H} \cong - \frac{\sqrt{M_\infty^2 - 1}}{\left(1 + \frac{\gamma-1}{2} M_\infty^2\right)} \frac{\varepsilon}{M_\infty} \tag{52}$$

where

$$M_e = M_\infty + \varepsilon \quad , \quad |\varepsilon| << M_\infty$$

Thus M_e takes the form of a dependent variable when Eqs. (51) and (52) are added to the set of Eqs. (36) - (38) .

VI. CONCLUDING REMARKS

Tani's two-moment integral method has been extended to treat non-adiabatic two-dimensional compressible boundary layers. The assumption of a "universal" stagnation enthalpy profile for all pressure gradients and wall temperatures is found to be quite accurate for attached boundary layers and provides a useful simplification. The accuracy of the integral method is found to be sensitive to the choice of the velocity profile. By use of the universal temperature profile and a carefully chosen one-parameter velocity profile the problem is reduced to solving two first order ordinary differential equations when the pressure gradient is prescribed. Predictions of the boundary layer properties and the separation point by this method compare favorably with "exact" numerical solutions.

Flow beyond the separation point is briefly considered. The "universal" temperature profile is no longer applicable. With the assumption of one-parameter families for temperature and velocity profiles, it is necessary to solve three first order ordinary differential equations. By comparing the present results with the reverse-flow Falkner-Skan profiles found by Cohen and Reshotko[28] one concludes that the separated flow velocity profiles in any integral method must be described either by a two-parameter family, or by the Falkner-Skan family itself. Another possibility is to use a multi-layer method.

REFERENCES

1. Falanga, R. A.; Hinson, W. F.; and Crawford, D. H.: Exploratory Tests of the Effects of Jet Plumes on the Flow over Cone-Cylinder Flare Bodies. NASA TN D-1000, February, 1962.

2. Bogdonoff, S. M. and Vas, I. E.: Hypersonic Separated Flows. Seventh Anglo-American Aeronautical Conference, New York, Oct. 5-7, 1959.

3. Chapman, Dean R.; Kuehn, Donald M.; and Larson, Harold K.: Investigation of Separated Flows in Supersonic and Subsonic Streams with Emphasis on the Effect of Transition. NACA Rep. 1356, 1958.

4. Beheim, Milton A.: Flow in the Base Region of Axisymmetric and Two-Dimensional Configurations. NASA TR R-77, 1960.

5. Tani, Itiro: Critical Survey of Published Theories on the Mechanism of Leading Edge Stall. Aero. Res. Inst., Univ. of Tokyo, Rep. No. 367, 1961.

6. Korst, H. H.; Page, R. H.; and Childs, M. E.: A Theory for Base Pressures in Transonic and Supersonic Flow. Univ. of Ill., Mech. Eng., Tech. Note 392-2, March, 1955.

7. Thwaites, B.: Approximate Calculation of the Laminar Boundary Layer. Aeronautical Quarterly, Vol. 1, pp. 245-280, May-Feb., 1949-1950.

8. Rott, N. and Crabtree, L. F.: Simplified Laminar Boundary Layer Calculations for Bodies of Revolution and for Yawed Wings. J. Aero. Sci., Vol. 19, No. 8, pp. 553-565, August, 1952.

9. Cohen, C. B. and Reshotko, E.: The Compressible Laminar Boundary Layer with Heat Transfer and Arbitrary Pressure Gradient. NACA TN 3326, 1955.

10. Libby, P. A. and Morduchow, M.: Method for Calculation of Compressible Laminar Boundary Layer with Axial Pressure Gradient and Heat Transfer. NACA TN 3157, 1954.

11. Beckwith, I. E.: Heat Transfer and Skin Friction by an Integral Method in the Compressible Laminar Boundary Layer with a Streamwise Pressure Gradient. NACA TN 3005, 1953.

12. Luxton, R. E. and Young, A. D.: Generalized Method for the Calculation of the Laminar Compressible Boundary Layer Characteristics with Heat Transfer and Non-Uniform Pressure Distribution. Brit. R. and M. No. 3233, 1962.

13. Curle, N.: The Effects of Heat Transfer on Laminar-Boundary Layer Separation in Supersonic Flow. Aeronautical Quarterly, Vol. 12, pp. 309-336, Nov., 1961.

14. Monaghan, R. J.: Effects of Heat Transfer on Laminar Boundary Layer Development under Pressure Gradients in Compressible Flow. Brit. R. and M. No. 3218, 1961.

15. Stewartson, K.: Further Solutions of the Falkner-Skan Equation. Proceedings of the Cambridge Philosophical Society, Vol. 50, p. 454, 1954.

16. Crocco, Luigi and Lees, Lester: A Mixing Theory for the Interaction Between Dissipative Flows and Nearly Isentropic Streams. J. Aero. Sci., Vol. 19, No. 10, Oct., 1952, pp. 649-676.

17. Bray, K. N. C.; Gadd, G. E.; and Woodger, M.: Some Calculations by the Crocco-Lees and Other Methods of Interactions between Shock Waves and Laminar Boundary Layers, including Effects of Heat Transfer and Suction. Brit. C. P. No. 556, 1961.

18. Glick, Herbert S.: Modified Crocco-Lees Mixing Theory for Supersonic Separated and Reattaching Flows. GALCIT Hypersonic Research Project, Memorandum No. 53, 1960.

19. Tani, Itiro: On the Approximate Solution of the Laminar Boundary Layer Equations. J. Aero. Sci., Vol. 21, No. 7, pp. 487-504, July, 1954.

20. Lees, Lester and Reeves, Barry L.: Some Remarks on Integral Moment Methods for Laminar Boundary Layers with Application to Separation and Reattachment. GALCIT Report, AFOSR 1920, December 31, 1961.

21. Chapman, Dean R.: A Theoretical Analysis of Heat Transfer in Regions of Separated Flow. NACA TN 3792, October, 1956.

22. Carlson, Walter O.: Heat Transfer in Laminar Separated and Wake Flow Regions. Proc. 1959 Heat Transfer and Fluid Mechanics Institute, Univ. of Calif., June, 1959.

23. Lankford, J. L.: The Effect of Heat Transfer on the Separation of Laminar Flow over Axisymmetric Compression Surfaces. U. S. Naval Ordnance Lab., NAVWEPS Rep. 7402, March, 1961.

24. Oswatitsch, K.: Die Ablösungsbedingung von Grenzschichten. Boundary Layer Research, Symposium Freiburg/Br. August 26-29, 1957. Edited by H. Görtler, Springer Verlag, 1950.

25. Goldstein, S.: On Laminar Boundary Layer Flow Near a Position of Separation. Quart. Journ. Mech. and Applied Math., Vol. 1, pp. 43-69, 1948.

26. Stewartson, K.: Correlated Incompressible and Compressible Boundary Layers. Proc. Royal Soc. (London), Ser. A, Vol. 200, No. A 1060, Dec. 22, 1949, pp. 84-100.

27. Poots, G.: A Solution of the Compressible Laminar Boundary Layer Equations with Heat Transfer and Adverse Pressure Gradient. Quart. Journ. Mech. and Applied Math., Vol. 13, Pt. 1, 1960.

28. Cohen, C. B. and Reshotko, E.: Similar Solutions for the Compressible Laminar Boundary Layer with Heat Transfer and Pressure Gradient. NACA Rep. 1293, 1956.

29. Margenau, H. and Murphy, G. M.: The Mathematics of Physics and Chemistry. D. Van Nostrand Company, Inc., Princeton, New Jersey, 1959.

30. Prandtl, L.: Z. Angew. Math. Mech., Vol. 18, pp. 77, 1938.

31. Meksyn, D.: Integration of the Boundary Layer Equations. Proceedings of the Royal Society, Series A, Vol. 237, pp. 543-559, 1956.

32. Meksyn, D.: New Methods in Laminar Boundary Layer Theory. Pergamon Press, New York, 1961.

TABLE 1

BOUNDARY LAYER FUNCTIONS $f(Y/\Delta)$ AND $g(Y/\Delta)$

Y/Δ	f	f'	g	g'
0	0	0	0	1.000
.1	.0191	.431	.0903	.779
.2	.094	1.095	.1505	.404
.3	.242	1.870	.1671	-.0864
.4	.460	2.41	.1351	-.522
.5	.699	2.22	.0739	-.629
.6	.882	1.334	.0207	-.374
.7	.958	.530	.0045	-.0635
.8	.988	.1315	0	0
.9	.996	.0474	0	0
1.0	1.000	0	0	0

TABLE 2

BOUNDARY LAYER INTEGRAL FUNCTIONS (ATTACHED FLOW, b = -1.99)

a	D	E	F	G	ℓnG	H	P	Q	W	Z
0	.4204	.09080	.1368	1.507	.4101	4.630	0	.9647	3.203	.3805
.25	.4041	.09681	.1453	1.501	.4061	4.174	.0484	.9590	3.005	.4078
.50	.3878	.10177	.1530	1.503	.4075	3.811	.1018	.9566	2.858	.4345
.75	.3716	.10568	.1596	1.511	.4128	3.516	.1585	.9582	2.752	.4617
1.00	.3553	.10854	.1651	1.521	.4194	3.273	.2171	.9681	2.681	.4900
1.25	.3390	.11034	.1693	1.534	.4279	3.072	.2759	.9860	2.636	.5206
1.50	.3227	.11109	.1721	1.549	.4376	2.905	.3333	1.0119	2.619	.5539
1.75	.3065	.11079	.1734	1.565	.4479	2.766	.3878	1.0501	2.626	.5913
2.00	.2902	.10944	.1731	1.582	.4587	2.652	.4378	1.0954	2.658	.6340
2.25	.2739	.10703	.1712	1.600	.4700	2.559	.4816	1.1477	2.718	.6831
2.50	.2576	.10357	.1674	1.616	.4800	2.487	.5179	1.2026	2.809	.7418
2.75	.2414	.09906	.1617	1.632	.4898	2.437	.5448	1.2554	2.936	.8126
3.00	.2251	.09350	.1540	1.647	.4990	2.407	.5610	1.3009	3.111	.9000

TABLE 3

PRESENT METHOD COMPARED WITH EXACT SOLUTION FOR SIMILAR "INCIPIENT SEPARATION" FLOW

S_w	$\frac{\delta_i^*}{X}\sqrt{\frac{m+1}{2}\frac{U_e X}{\nu_\infty}}$		$\frac{\theta_i}{X}\sqrt{\frac{m+1}{2}\frac{U_e X}{\nu_\infty}}$		$\frac{\xi}{X}\sqrt{\frac{m+1}{2}\frac{U_e X}{\nu_\infty}}$		$-\frac{S_w'}{S_w}$	
	present method	NACA Rep. 1293	present method	NACA Rep. 1293	present method	NACA Rep. 1293	present method	NACA Rep. 1293
-1.0	.92	1.3200	.655	.6400	-2.12	-2.1395	.275	.2477
-0.8	1.29	1.4052	.625	.6274	-1.61	-1.5211	.289	.2826
-0.4	2.00	1.8383	.595	.6045	- .762	- .6942	.303	.3123
+1.0	4.38	3.8162	.556	.5677	1.798	1.6109	.325	.3388

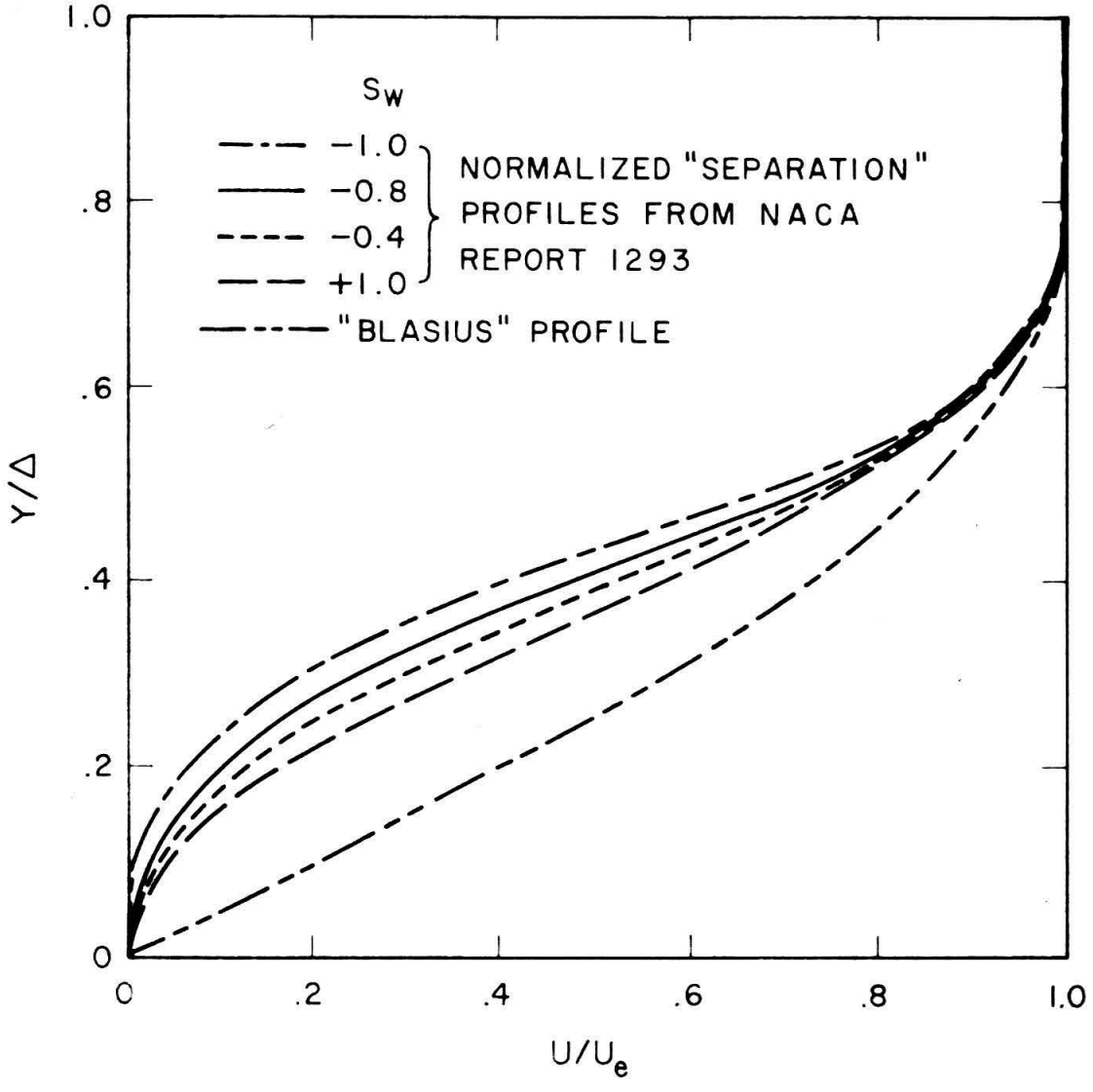

FIGURE 1

SIMILARITY SEPARATION VELOCITY PROFILES

IN THE INCOMPRESSIBLE PLANE

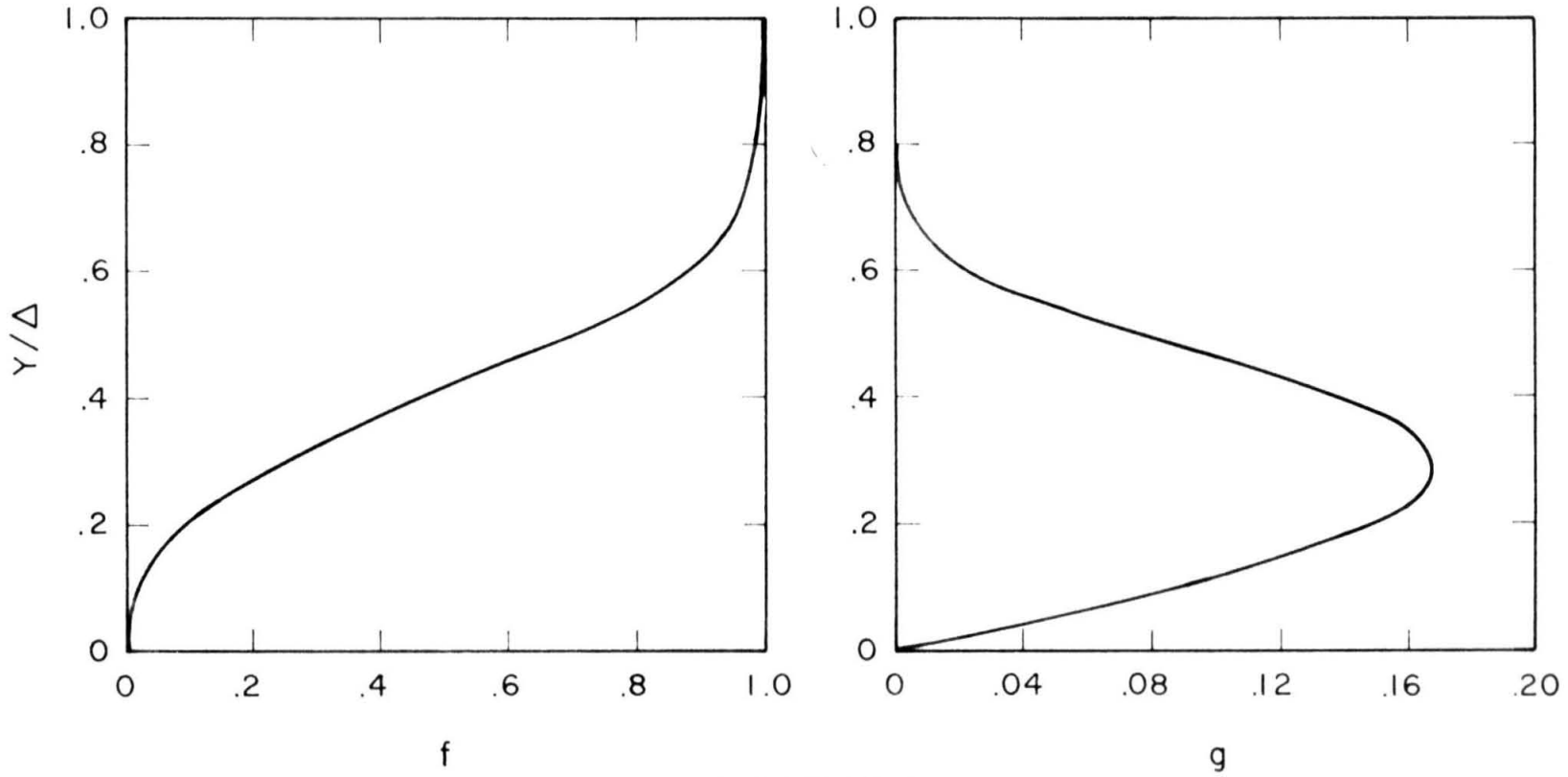

FIGURE 2

BOUNDARY LAYER FUNCTIONS "f" AND "g"

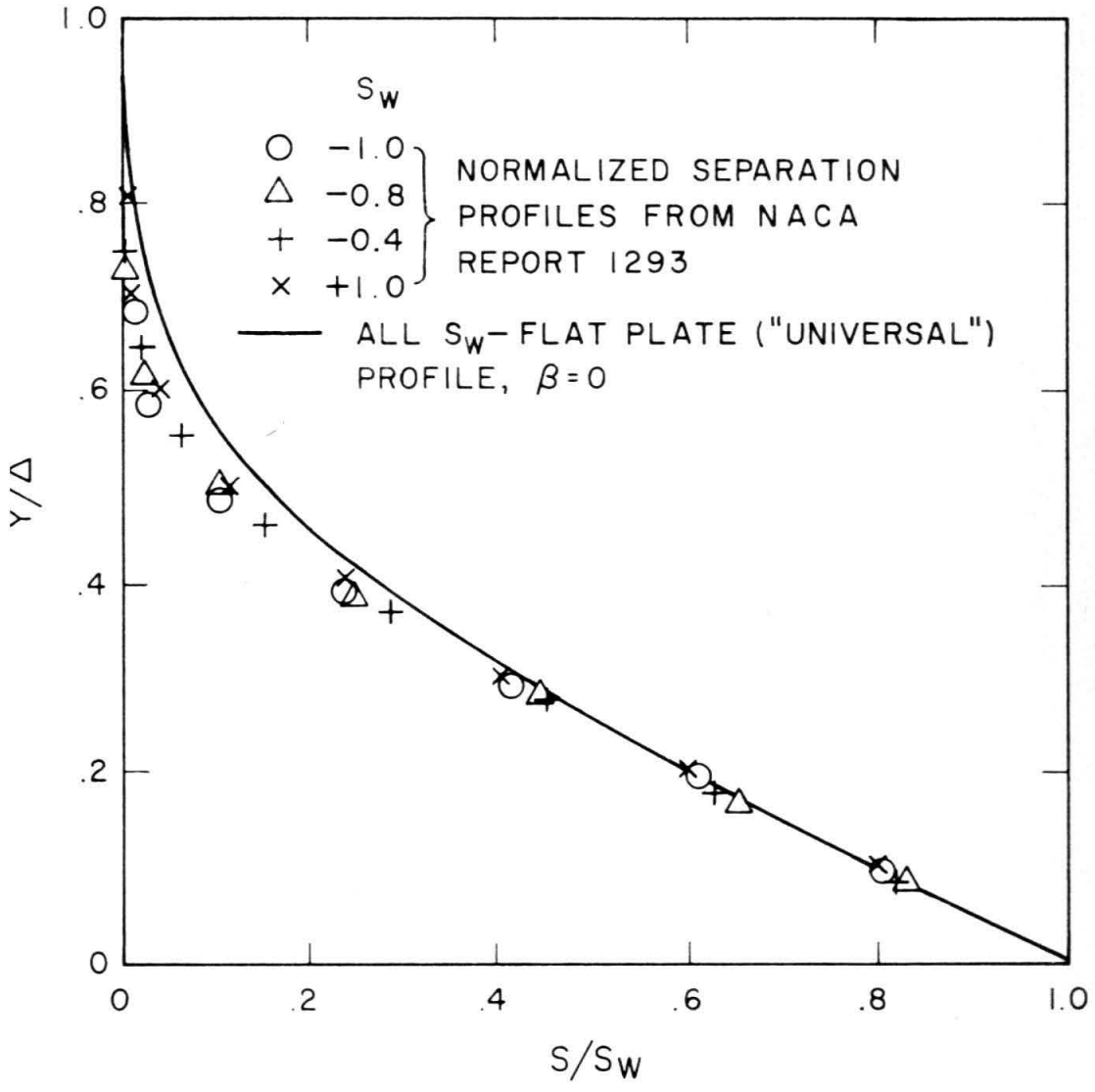

FIGURE 3

SIMILARITY TOTAL TEMPERATURE PROFILES

IN THE INCOMPRESSIBLE PLANE

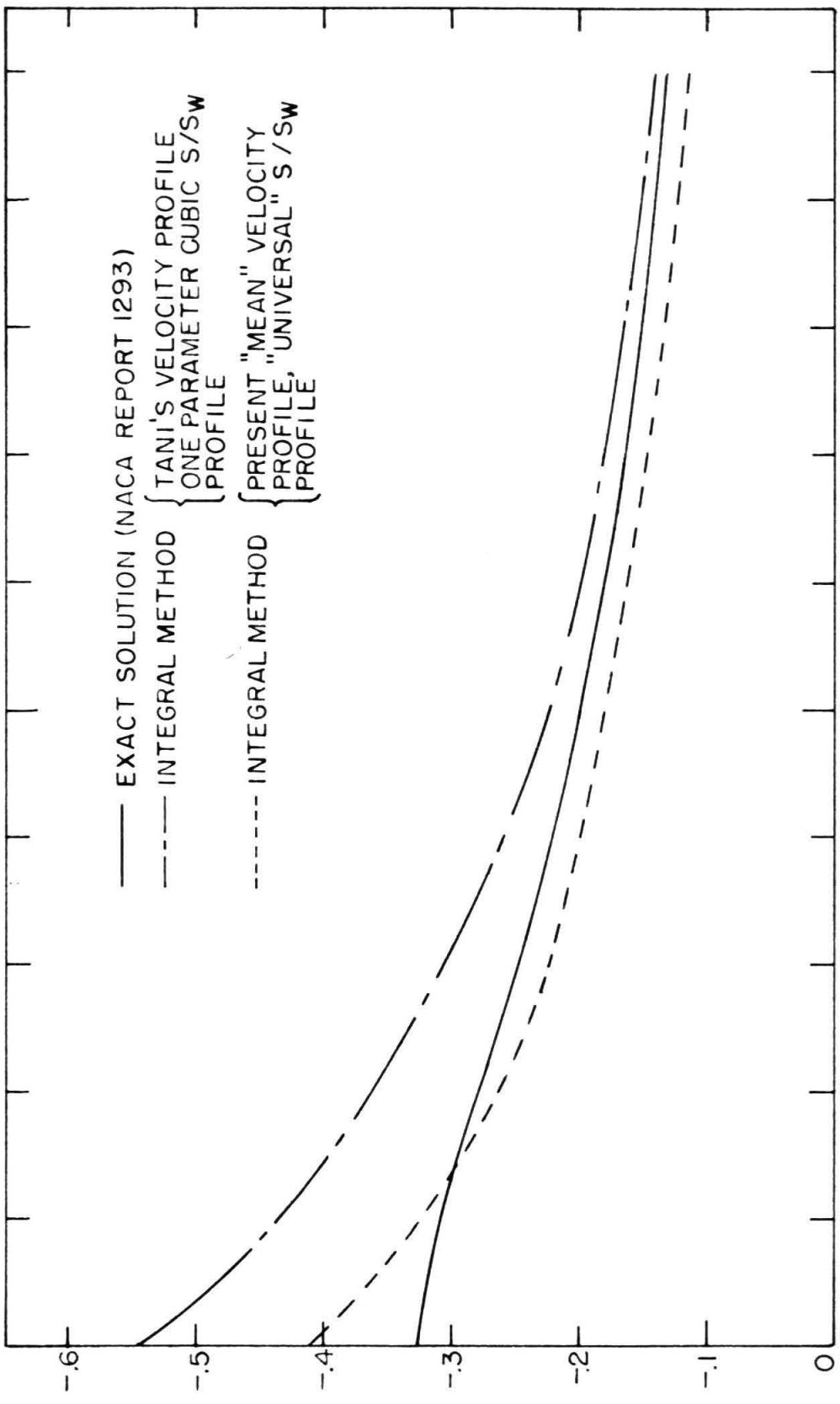

FIGURE 4

PRESSURE GRADIENT PARAMETER VS. WALL TEMPERATURE FOR SIMILARITY SEPARATION FLOW

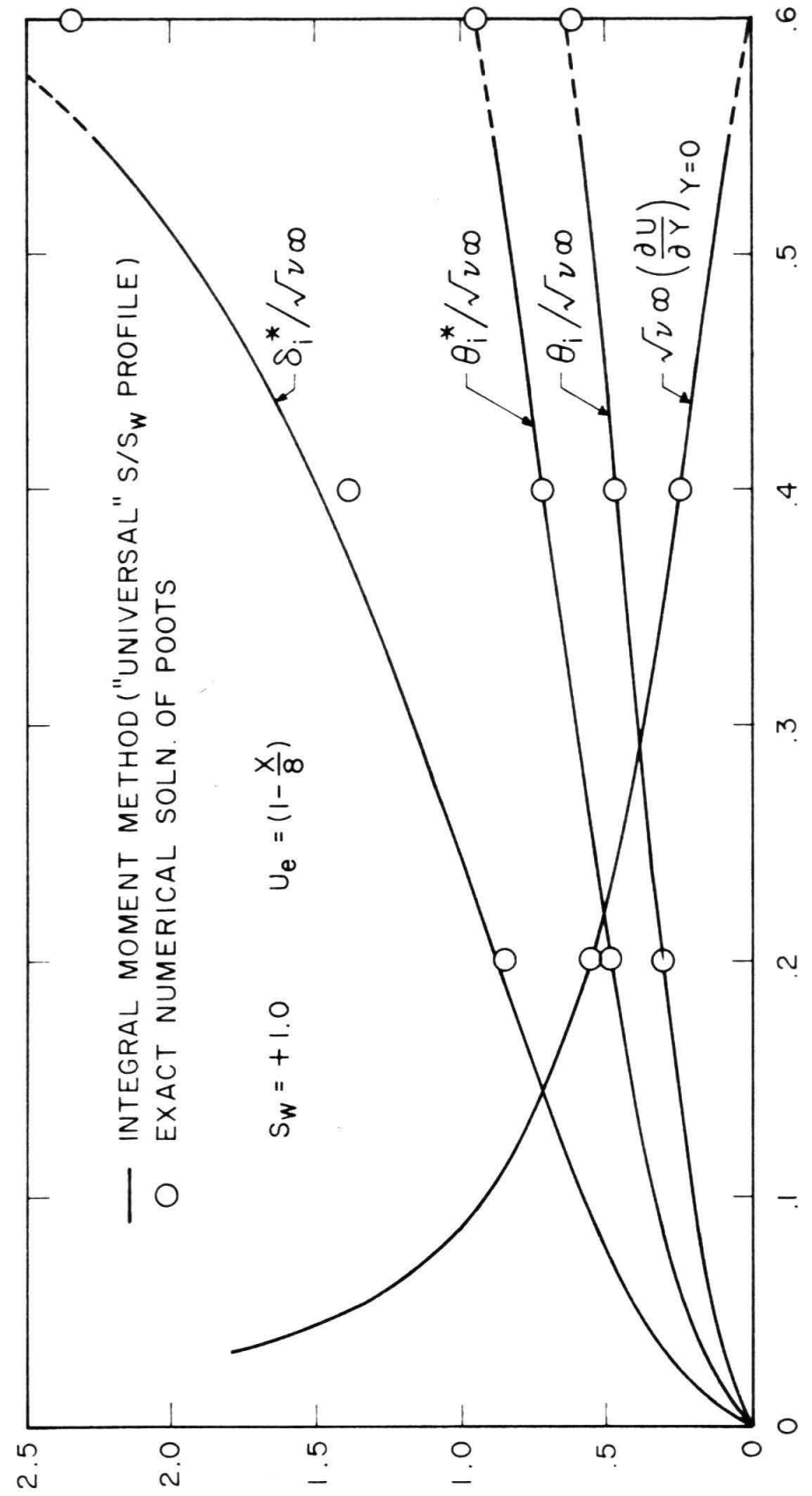

FIGURE 5

VELOCITY BOUNDARY LAYER CHARACTERISTICS

IN INCOMPRESSIBLE PLANE FOR $S_w = +1.0$

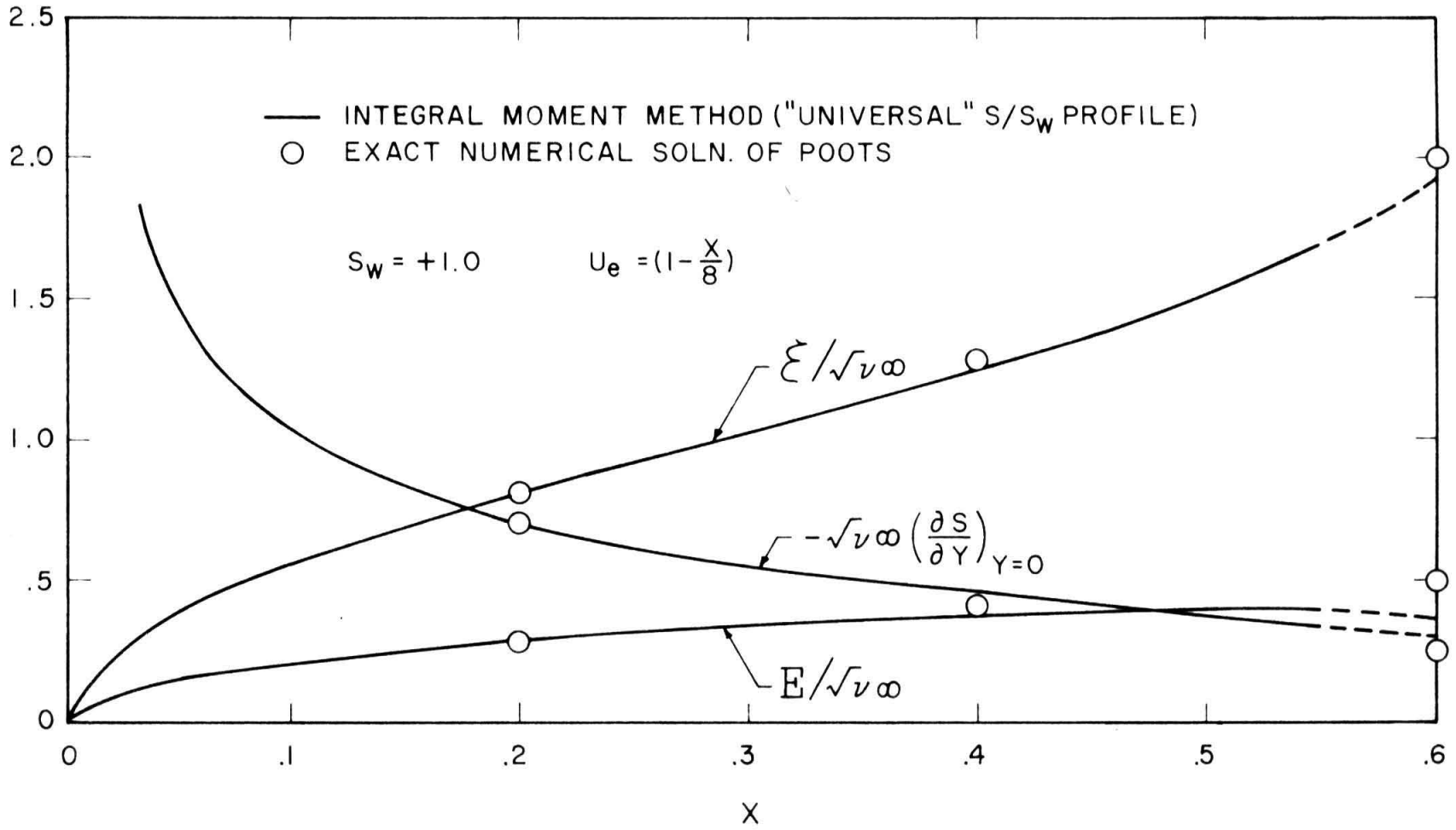

FIGURE 6

THERMAL BOUNDARY LAYER CHARACTERISTICS

IN INCOMPRESSIBLE PLANE FOR $S_w = +1.0$

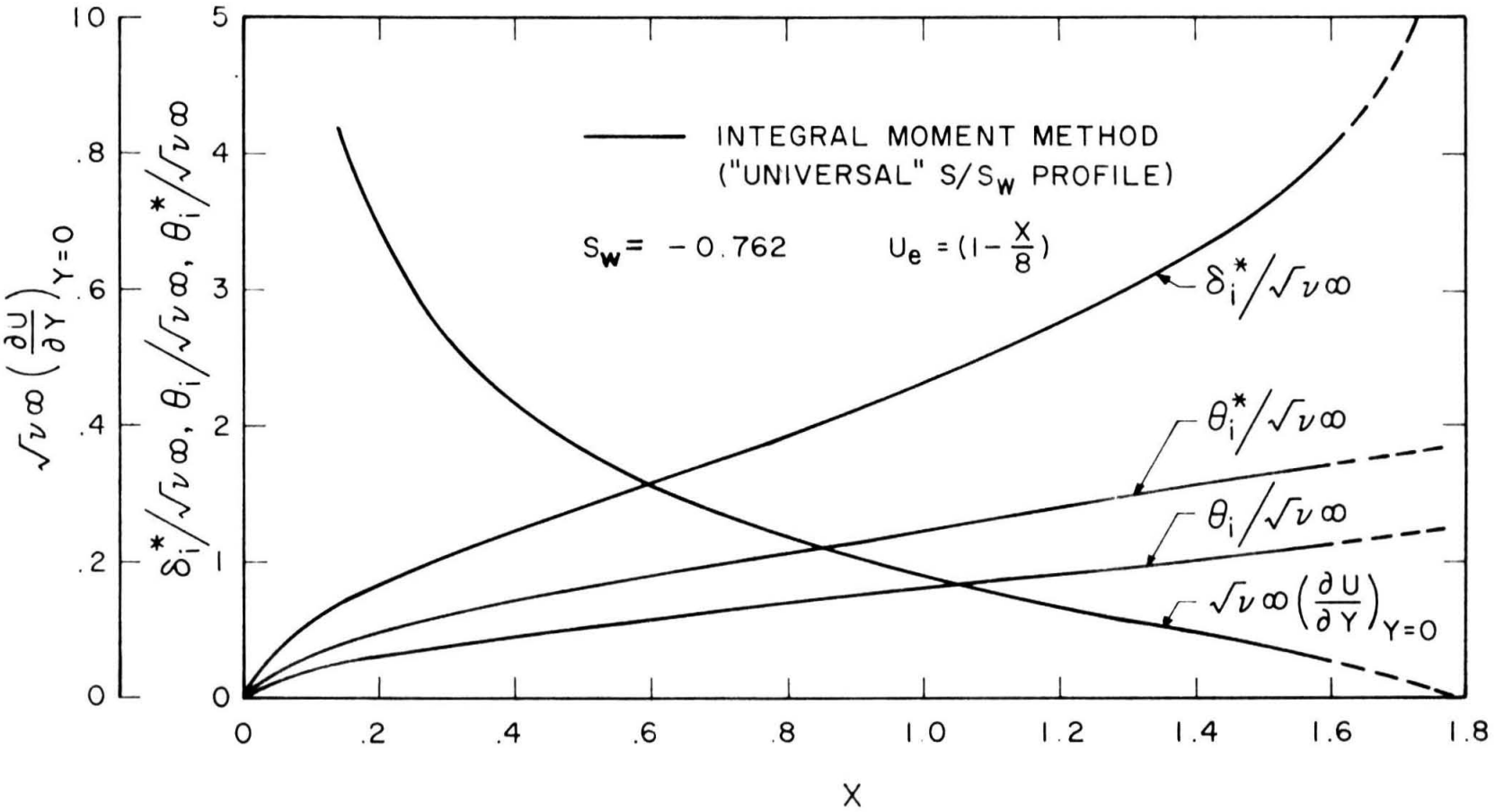

FIGURE 7

VELOCITY BOUNDARY LAYER CHARACTERISTICS

IN INCOMPRESSIBLE PLANE FOR S_w = - 0.762

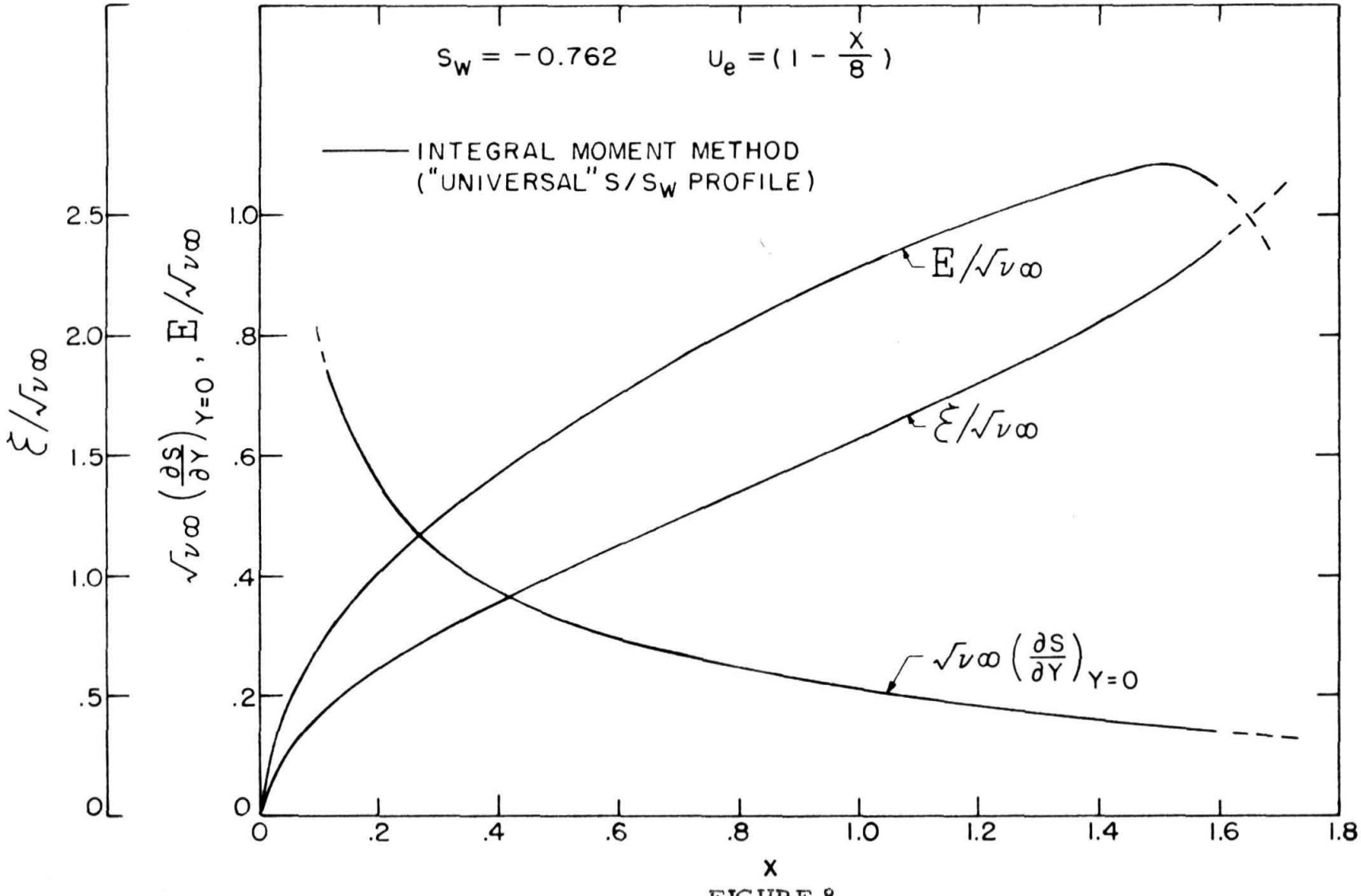

FIGURE 8

THERMAL BOUNDARY LAYER CHARACTERISTICS

IN INCOMPRESSIBLE PLANE FOR $S_w = -0.762$

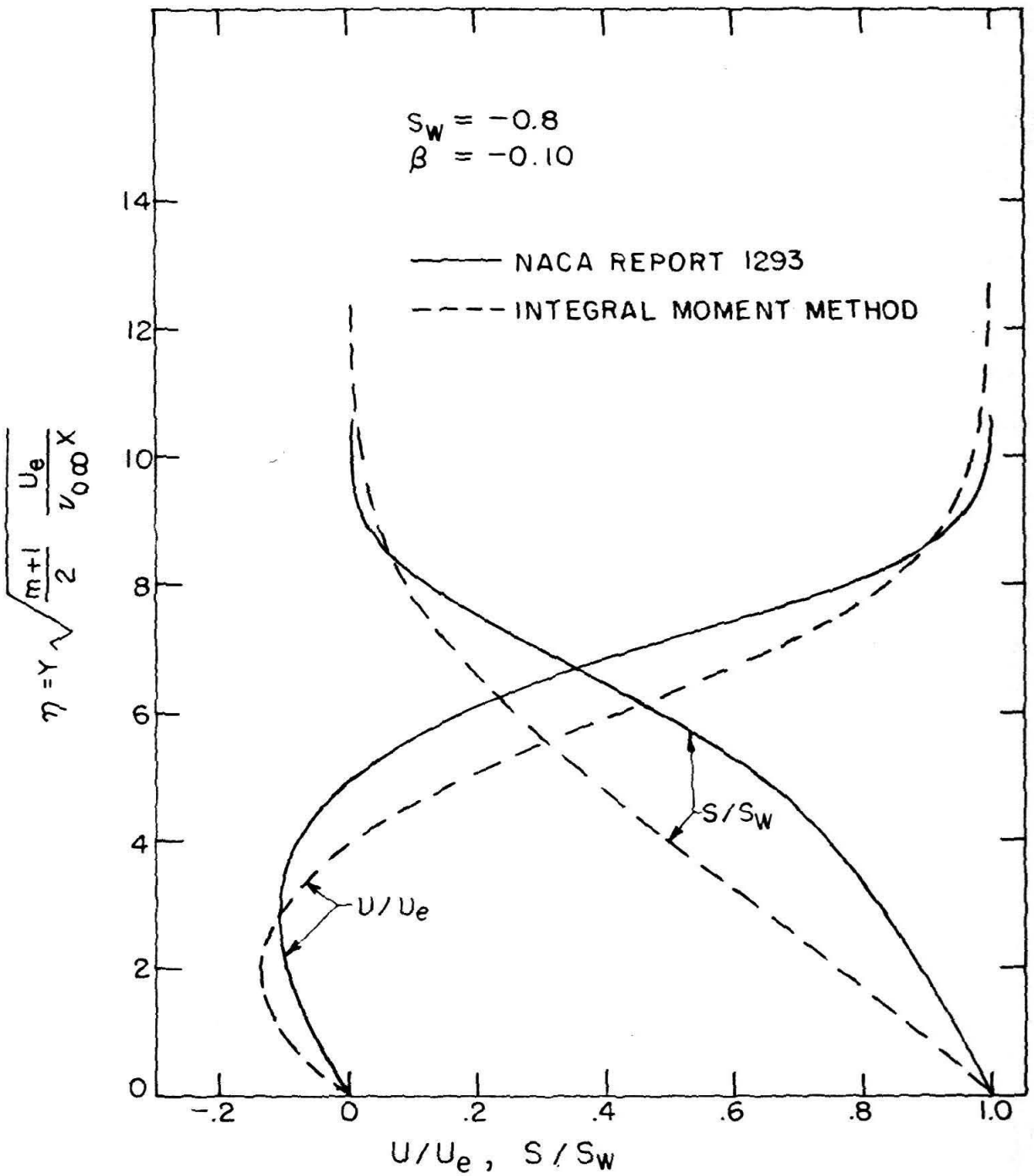

FIGURE 9

COMPARISON OF VELOCITY AND TEMPERATURE PROFILES FOR SEPARATED SIMILARITY FLOW